

Magnetically induced oscillations of the spin polarization in the Datta–Das geometry

Andriy H. Nevidomskyy* and Karyn Le Hur

Département de Physique, Université de Sherbrooke, Sherbrooke, Québec, J1K 2R1, Canada

(Dated: February 8, 2020)

The control of intrinsic magnetic degrees of freedom is very important as it offers a practical means to manipulate and probe electron spin transport. Tunable spin-orbit effect in quantum wires can in principle serve as a means to achieve this goal. Here, we investigate within the scattering matrix approach the effect of an in-plane magnetic field on the conductance of a quantum wire in the Datta–Das geometry and show that the interplay of the spin-orbit interaction with the magnetic field provides enhanced control over the electron spin polarization. In particular, we predict a novel effect of magnetically induced oscillations of the electron spin in a certain range of magnetic field.

PACS numbers: 71.70.Ej, 72.25.-b, 72.25.Dc, 73.63.Nm

Spin effects in transport embody a new branch in mesoscopic physics and semiconductor spintronics [1] with several technological applications such as information storage, magnetic sensors, and potentially quantum computation [2]. One of the first devices that would control the electron spins was proposed by Datta and Das [3] who suggested the use of the gate-controlled Rashba spin-orbit interaction [4] as a means of varying the spin polarization in one-dimensional quantum wires. The use of the Rashba interaction in beam-splitter devices and its effect on the shot noise have also been envisioned in the context of quantum entanglement [5]. The combined effect of the Zeeman field and spin-orbit coupling has been the subject of a number of recent works [6, 7, 8], however they have concentrated on the band structure issues [7] or on the effect of the interactions on the spectrum of collective excitations [6, 8], whereas an important question of the effect of the magnetic field on the transmission of the Datta–Das setup has not been investigated so far.

Here we consider the Datta–Das setup [3] that consists of a quantum wire with the Rashba [4] spin-orbit interaction (region II in Fig. 1) coupled to the ferromagnetic leads (regions I and III), so that a spin-polarized current can be injected from the left and drained on the right. The whole setup, including the leads, is then put into an in-plane magnetic field, allowing us to avoid orbital as well as the Aharonov–Bohm effects [9, 10] that would have occurred if the field were perpendicular to the device plane. Applying the scattering matrix formalism, we demonstrate that the interplay of the magnetic field with the spin-orbit effect gives rise to the novel spin oscillations that can be exploited to enhance the control over the electron spin-polarization in the Datta–Das geometry.

The spin-orbit coupling is a relativistic effect [11] resulting in the Hamiltonian $\hat{H}_{SO} \propto \nabla V \cdot (\hat{\sigma} \times \hat{p})$, where \hat{p} is the electron momentum, $\hat{\sigma}$ are the Pauli matrices and V is the electrostatic potential. It has been shown that in most two-dimensional heterostructures [12, 13] on which the Datta–Das device is based, the Dresselhaus spin-orbit effect due to the microscopic crystal field [14] is much smaller compared to the Rashba effect caused by

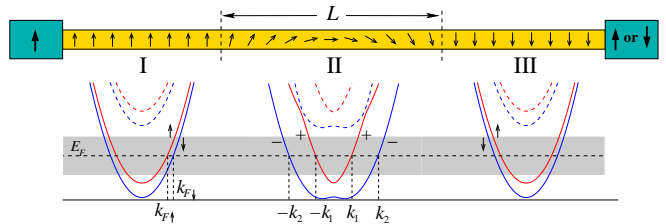


FIG. 1: Datta–Das geometry and the sketch of the energy band structure in the applied magnetic field. The Rashba-active region of length L comprises the middle part of the wire. In the energy dispersion plots, two transverse bands (solid and broken lines) are shown, however the discussion is limited to the position of the Fermi level, E_F , in the grey region, where only the lowest transverse channel is active.

the quantum-well asymmetry. Therefore we shall limit our discussion to the Rashba Hamiltonian [4]:

$$\hat{H}_R = \alpha(\hat{\sigma} \times \hat{p})_z/\hbar = i\alpha(\hat{\sigma}_y \partial_x - \hat{\sigma}_x \partial_y). \quad (1)$$

The constant α absorbs in itself the electric field normal to the semiconductor interface and takes value in the range $(1-10) \times 10^{-10}$ eV cm for a large variety of systems (InAs/GaSb [15], $In_x Ga_{1-x} As / In_x Al_{1-x} As$ [12, 16] and GaAs/ $Al_x Ga_{1-x} As$ [17]) depending on the shape of the confining quantum well. The energy scale of the Rashba spin-orbit interaction is given by $E_{SO} = \hbar^2 k_R^2 / 2m^* = \alpha^2 m^* / 2h^2$ and is of the order of $10^{-4} - 10^{-2}$ meV, where $k_R = \alpha m^* / \hbar^2$ is the characteristic Rashba wave-vector.

Let us consider the case of zero magnetic field first. For electrons moving along the wire in the region II in Fig. 1 we have $p_y = 0$ and the Rashba term $H_R = \alpha \hat{\sigma}_y \hat{p}_x / \hbar$. Hence the electrons with opposite projections of the $\hat{\sigma}_y$ component of the spin correspond to the different Rashba-split dispersion branches with different Fermi wave-vectors k_1 and k_2 . They will thus pick up different phases in the Rashba region of length L , and the transmission probability will be governed by the phase difference $(k_2 - k_1)L$. It is equal to $2\theta_R \equiv 2k_R L = 2\alpha L m^* / \hbar^2$ and is proportional to the spin-orbit strength α . For the equal spin-polarizations of the source and drain, say, the transmission of the wire reads [3]: $T_{\uparrow\uparrow} = \frac{1}{2}(1 + \cos 2\theta_R)$.

Model. In this work we shall consider the effect that the in-plane magnetic field B has on the transmission of

the Datta-Das setup. We start from the Hamiltonian

$$\hat{H} = \frac{\hat{p}^2}{2m^*} - \frac{\alpha}{\hbar} \hat{\sigma}_y \hat{p}_x + \Delta \hat{\sigma}_x + V_c(y) + \frac{\alpha}{\hbar} \hat{\sigma}_x \hat{p}_y, \quad (2)$$

where the Zeeman energy $\Delta = g\mu_B B/2$, and $V_c(y)$ is the lateral confining potential perpendicular to the wire.

For narrow enough wires the electron momentum is aligned mostly with the direction of the wire, so that $\langle p_x \rangle \gg \langle p_y \rangle$, and we shall neglect the last spin-orbit term in the Hamiltonian (2). This results in a simple picture shown schematically in Fig. 1 of a number of non-interacting transverse subbands with energies E_n^y that can be obtained by diagonalizing the y -dependant part of the Hamiltonian. It has been demonstrated [18, 19] however that this approximation breaks down in the vicinity of the crossing of the transverse subbands, since the spin-orbit interaction would mix different transverse channels and lift the subband degeneracy, leading to the band anticrossing. Egues, Burkard and Loss [20] have shown that this anticrossing can be exploited in the Datta-Das setup to enhance the spin control. Here we shall consider the realm of only the lowest subband, which can be achieved by tuning the gate voltage so that the Fermi level lies in the shaded region of the energy dispersion in Fig. 1.

The Hamiltonian (2) can be written as a matrix in the spin-space and its eigenvalues are given by $E_{\pm}(k) = \frac{\hbar^2 k^2}{2m^*} \pm \sqrt{\Delta^2 + \alpha^2 k^2}$. Here we consider two limits, $\Delta \gg E_{\text{so}}$ and $E_{\text{so}} \gg \Delta$, that allow analytical solutions.

Case $\Delta \gg E_{\text{so}}$. We find it convenient to introduce the dimensionless ratio $\gamma = E_{\text{so}}/\Delta$. When $\gamma \ll 1$ the expression for eigen-energies above can be simplified as:

$$E_{\pm}(k) \approx \frac{\hbar^2 k^2}{2m^*} (1 \pm 2\gamma) \pm \Delta + \mathcal{O}(\gamma^2). \quad (3)$$

Furthermore, the corresponding eigenfunctions yield the following spinor form in the basis of $|\uparrow\rangle$ and $|\downarrow\rangle$ states (defined along the magnetic field axis chosen to be z here)

$$\begin{aligned} |\psi_-(k)\rangle &= \frac{1}{\sqrt{1+\gamma^2 k^2/k_R^2}} \begin{pmatrix} -i\gamma k/k_R \\ 1 \end{pmatrix} e^{ikx} \\ |\psi_+(k)\rangle &= \frac{1}{\sqrt{1+\gamma^2 k^2/k_R^2}} \begin{pmatrix} 1 \\ -i\gamma k/k_R \end{pmatrix} e^{ikx}. \end{aligned} \quad (4)$$

We aim to obtain the scattering matrix of the system from the continuity conditions for the wave-functions and their first derivatives at the boundary between regions I and II, and II and III of the wire (see Fig. 1). The solution in the Rashba-active region is a linear combination of $|\psi_-\rangle$ and $|\psi_+\rangle$, whereas in regions I and III, where only the Zeeman term is present, it is given by spinors $|\uparrow\rangle$ and $|\downarrow\rangle$. In the latter regions the Fermi wave-vectors are $k_{F_{\uparrow,\downarrow}} = k_0 \sqrt{1 \mp \Delta/E_F}$, where $k_0 = \sqrt{2m^* E_F}/\hbar$ is the Fermi wave-vector without magnetic field, and $\Delta \ll E_F$ is assumed throughout. The corresponding Fermi velocities are given by $v_{F_{\uparrow,\downarrow}} = v_0 \sqrt{1 \mp \Delta/E_F}$, whereas for the Rashba-active region II we obtain $k_{1,2} = k_{F_{\uparrow,\downarrow}}/\sqrt{1 \pm 2\gamma}$.

Resorting to the above expressions for the wave-vectors and velocities at the Fermi level, one obtains the scattering matrix following a standard procedure [3, 20]. The transmission coefficient for the equal-spin polarizations in both leads is readily expressed through the elements of the scattering matrix (neglecting higher orders in γ):

$$\begin{aligned} T_{\uparrow\uparrow} = T_{\downarrow\downarrow} &\approx 1 - \frac{4\beta_1\beta_2}{(1+\beta_1\beta_2)^2} \sin^2 \left[\frac{(k_2 - k_1)L}{2} \right] \quad (5) \\ &\approx 1 - \frac{4\beta_1\beta_2}{(1+\beta_1\beta_2)^2} \sin^2 \left[\left(\frac{\Delta}{2E_F} + \gamma \right) k_0 L \right], \end{aligned}$$

where the coefficients $\beta_{1,2}$ are given by

$$\beta_{1,2} \equiv \frac{\gamma k_{1,2}}{k_R} \approx \frac{\sqrt{E_{\text{so}} E_F}}{\Delta} \left(1 \mp \frac{\Delta}{2E_F} \mp \gamma \right). \quad (6)$$

The argument of the sine in Eq. (5) is the phase shift between the two subbands, similar to the original Datta-Das setup. However unlike in the former case, the magnetic field enters Eq. (5) through the Fermi wave-vectors $k_{1,2}$, leading to the oscillations of the transmission with the field strength Δ . It is important to distinguish these oscillations from the well-known Aharonov-Bohm effect [9] and the spin-orbit induced Berry phase [10] that stem from the electron wave-function acquiring a phase along a closed trajectory in the magnetic field.

It is evident from Eqs. (5) and (6) that in the absence of Rashba effect, $E_{\text{so}} \rightarrow 0$, the prefactor in front of the sine vanishes and $T_{\uparrow\uparrow} \rightarrow 1$, as it should be for the fully spin-polarized case. The physical meaning of Eq. (5) is thus clear: it describes the deviation from the perfect transmission caused by a finite Rashba interaction.

Similarly, one can write down the expressions for the cross-channel transmissions, i.e. for the opposite spin-polarizations in the left and right leads [21]:

$$\begin{aligned} T_{\uparrow\downarrow} &= \frac{4\beta_1^2}{(1+\beta_1\beta_2)^2} \left(\frac{v_{F\uparrow}}{v_{F\downarrow}} \right) \sin^2 \left[\frac{(k_2 - k_1)L}{2} \right] \\ T_{\downarrow\uparrow} &= \frac{4\beta_2^2}{(1+\beta_1\beta_2)^2} \left(\frac{v_{F\downarrow}}{v_{F\uparrow}} \right) \sin^2 \left[\frac{(k_2 - k_1)L}{2} \right]. \end{aligned} \quad (7)$$

Here $T_{\uparrow\downarrow} \neq T_{\downarrow\uparrow}$ due to the different Fermi velocities and wave-vectors of the two subbands (see Fig. 1).

The dependence of $T_{\uparrow\uparrow}$ on the strength of the Rashba constant α is shown in Fig. 2 for several values of $\nu \equiv 1/\gamma$, where we chose $E_F = 0.1$ eV along the lines of Ref. [16] and the length of the wire $L = 400$ nm. $T_{\uparrow\uparrow}(\alpha)$ is an oscillating function with a striking dependence of both the amplitude and the period on the magnetic field.

Most importantly, instead of varying the strength of the Rashba interaction α by gating the Datta-Das device, as has been proposed originally[3], our setup offers another efficient way of controlling the current spin polarization by means of varying the applied magnetic field. The dependence of the transmission $T_{\uparrow\uparrow}$ on the magnetic field $\nu \equiv \Delta/E_{\text{so}}$ is shown with the solid line in Fig. 3.

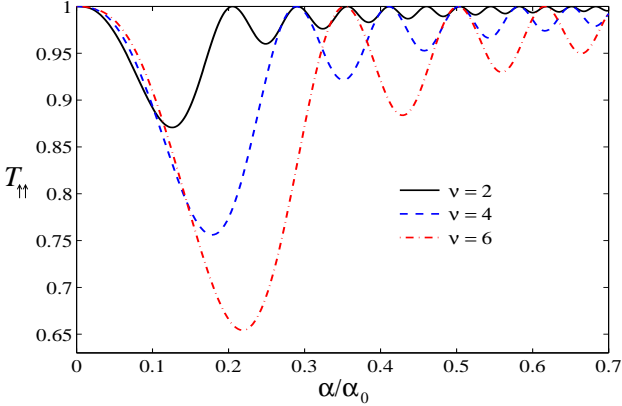


FIG. 2: Transmission $T_{\uparrow\uparrow}$ in the equal-spin channel of the Datta-Das device as a function of the Rashba coefficient α . Three different values of the applied magnetic field $\nu \equiv \Delta/E_{\text{so}} > 1$ have been considered, as shown in the legend.

Let us analyze in more detail the phase shift in Eq. (5):

$$\frac{(k_2 - k_1)L}{2} \approx k_0 L \left(\frac{\Delta}{2E_F} + \gamma \right) \propto (\varepsilon_{\text{so}}\nu + 1/\nu), \quad (8)$$

where $\varepsilon_{\text{so}} \equiv E_{\text{so}}/2E_F$. At small values of $1 \ll \nu < \nu_0$, with $\nu_0 \equiv \sqrt{1/\varepsilon_{\text{so}}}$, the second term in Eq. (8) dominates and the transmission is governed by the term $\sin^2(k_0L/\nu)$, hence the period of oscillations becoming smaller as ν decreases (inset in Fig. 3). For large values of ν the linear term in (8) prevails, leading to the constant period $1/\varepsilon_{\text{so}}$ of oscillations. Their amplitude is governed by the prefactor of the sine in Eq. (5), whose dependence on ν is shown in broken line in Fig. 3.

Let us estimate the value of magnetic field B_R when the Zeeman splitting is equal to the Rashba energy (i.e. $\gamma = 1$). Taking the value of $\alpha_0 = 7 \times 10^{-10}$ eV cm, as determined for the InGaAs/InAlAs interface in Ref. [16], we obtain the spin-orbit energy $E_{\text{so}} = 1.6 \times 10^{-5}$ eV, which, given the electron g-factor $g = 4$, corresponds to the magnetic field $B_R = 0.14$ T. The optimal value of the magnetic field for the situation shown in Fig. 3 is $\nu_0 \approx 40$, corresponding to the magnetic field $B_0 = \nu_0 B_R \approx 5.6$ T, which lies in the experimentally available range.

Case $E_{\text{so}} \gg \Delta$. We now turn our attention to the opposite limit of dominant Rashba interaction and small Zeeman perturbation ($\nu \equiv \Delta/E_{\text{so}} \ll 1$). We shall construct a perturbative scheme starting from the $\nu = 0$ (pure Rashba) Hamiltonian in the basis of plane waves: $H_x = \frac{\hbar^2 k^2}{2m^*} - \alpha \hat{\sigma}_y k$, where, as before, we have limited ourselves to only the lowest transverse subband. For $\nu = 0$ the eigenvalues are $\varepsilon_{\pm} = \frac{\hbar^2 k^2}{2m^*} \mp \alpha k$ and the corresponding eigenfunctions $|+\rangle_y, |-\rangle_y$ are the eigenstates of $\hat{\sigma}_y$.

In terms of these eigenstates, the matrix elements of the Zeeman perturbation, $V \equiv \Delta \hat{\sigma}_x$, are equal to ${}_y\langle -|V|+\rangle_y = -{}_y\langle +|V|- \rangle_y = i\Delta$. Solving the resulting Hamiltonian at the 2nd order of the perturbation theory, we obtain eigenvalues $E_{\pm} \approx \varepsilon_{\pm} \pm \frac{\Delta^2}{\varepsilon_{+} - \varepsilon_{-}} \equiv \varepsilon_{\pm} \mp (\frac{\varkappa}{k})\Delta$, where $\varkappa = \frac{\Delta}{2\alpha} \equiv k_R \nu / 4$ is a characteristic wave-vector

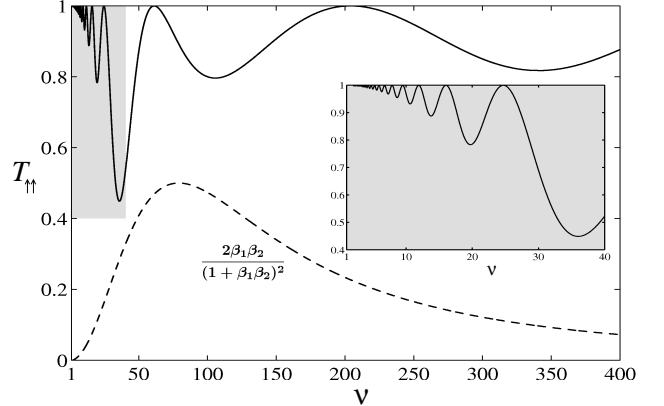


FIG. 3: Transmission of the Datta-Das device $T_{\uparrow\uparrow}$ (solid line), as a function of magnetic field $\nu = \Delta/E_{\text{so}} \gg 1$. The Rashba constant $\alpha = \alpha_0$ was assumed as for InGaAs/InAlAs interface in Ref. [16]. The inset shows the details of the behaviour of $T_{\uparrow\uparrow}$ at low magnetic fields, in the shaded region of the main plot. The dashed curve traces the dependence of the numerical prefactor in front of $2 \sin^2[(k_2 - k_1)L/2]$ in $T_{\uparrow\uparrow}$.

with the effective kinetic energy $\frac{\hbar^2 \varkappa^2}{2m^*} = \nu E_{\text{so}}/4 \equiv \Delta/4$.

Of course, the perturbation theory is only valid when the correction $\delta E = \Delta(\varkappa/k)$ is small compared to bare Rashba energies ε_{\pm} , which translates into $k \gg \varkappa$. Therefore, in order for the perturbation theory to be applicable, the Fermi level has to be higher than $E_{F_{\text{min}}} \approx 2\Delta$.

The eigenstates of the problem at the second order of the perturbation theory in Δ yield the forms

$$|+\rangle = |+\rangle_y - i\frac{\varkappa}{k} |-\rangle_y \equiv \frac{1}{\sqrt{2(1 + \varkappa^2/k^2)}} \begin{pmatrix} 1 - i\varkappa/k \\ i - \varkappa/k \end{pmatrix} \quad (9)$$

$$|-\rangle = |-\rangle_y + i\frac{\varkappa}{k} |+\rangle_y \equiv \frac{1}{\sqrt{2(1 + \varkappa^2/k^2)}} \begin{pmatrix} 1 + i\varkappa/k \\ -i - \varkappa/k \end{pmatrix}.$$

We note that the bands described by these states are not continuous at $k = 0$, since the perturbation theory is not applicable there. Consequently, the right-moving carriers at the Fermi level with $k = k_2$ are described by the $|+\rangle_{k_2}$ state, whereas the left-moving carriers with the opposite momentum are described by the $|-\rangle_{-k_2}$ state. Here the Fermi wave-vectors of the Rashba subbands are given by

$$k_{1,2} = k_0 \mp k_R + \mathcal{O}\left(\frac{E_{\text{so}}}{E_F}, \frac{\Delta^2}{E_F E_{\text{so}}}\right) \approx k_0(1 \mp \beta), \quad (10)$$

where $\beta \equiv k_R/k_0 = \sqrt{2\varepsilon_{\text{so}}}$ and we neglected the higher order terms in the last equality. Using Eqs. (9–10), it is a straightforward though tedious task to write down the boundary conditions between the Rashba-active and Zeeman-only regions and obtain the scattering matrix. The final result for $T_{\uparrow\uparrow}$ is given in full in the endnote [22].

The dependence of $T_{\uparrow\uparrow}$ on the Rashba coupling constant α is illustrated in Fig. 4a. For small magnetic fields ν , the curve is almost indistinguishable from the cosine (dash-dotted line in Fig. 4a). Indeed, one can Taylor-expand $T_{\uparrow\uparrow}(\nu)$ around $\nu = 0$ to obtain, up to linear order,

$$T_{\uparrow\uparrow}(\nu) \approx \cos^2 \theta_R - \sin^2 \theta_R (2 \cos^2 \theta_R - \eta \sin 2\theta_R \cot \phi) \nu, \quad (11)$$

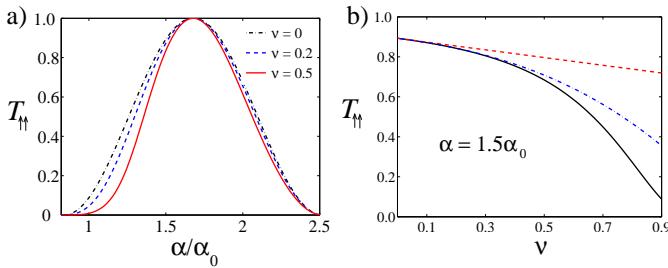


FIG. 4: Transmission of the Datta-Das device, $T_{\uparrow\uparrow}$, in the limit of weak magnetic field $\nu = \Delta/E_{\text{so}} \ll 1$ as a function of (a) the Rashba coefficient α , for three different values of magnetic field (see legend); (b) the magnetic field ν for a fixed value of $\alpha = 1.5\alpha_0$. The value of α_0 is for the InGaAs/InAlAs interface [16]. In panel (b), the linear approximation Eq. (11) for $T_{\uparrow\uparrow}(\nu)$ is plotted in broken line; the dash-dotted line shows the Taylor expansion of $T_{\uparrow\uparrow}(\nu)$ up to cubic order in ν .

where the angle $\phi \equiv k_0 L (1 + \varepsilon_{\text{so}})$ and η is a spin-orbit dependant constant $\eta \equiv \frac{\beta}{2} \frac{1 + \varepsilon_{\text{so}}}{(1 + \varepsilon_{\text{so}})^2 - \beta^2}$. Therefore for zero magnetic field we find $T_{\uparrow\uparrow}|_{\nu=0} = \frac{1}{2}(1 + \cos 2\theta_R)$, in agreement with the conventional Datta-Das formula.

The dependence of $T_{\uparrow\uparrow}$ on ν is plotted in Fig. 4b in solid line. The linear fit of Eq. (11) is shown in broken line, and serves as a good approximation for $\nu \lesssim 0.2$. This regime, $\Delta \ll E_{\text{so}}$, turns out to be less interesting from the application point of view since the only effect of the magnetic field is to monotonously suppress the transmission coefficient $T_{\uparrow\uparrow}$ (see Fig. 4b), as opposed to the ubiquitous oscillating behaviour found for large fields.

Conclusions. We have investigated the interplay between the Rashba spin-orbit interaction and Zeeman effect in quantum wires in the Datta-Das geometry, exploiting the scattering matrix approach. The conventional setup, without an external magnetic field, permits in principle to control the electron spin polarization by means of variable spin-orbit interaction α . However, it has a limited application in practice since the range of variation of α is quite narrow [16]. By adding an in-plane magnetic field to the setup, we have shown that the prolific combination of the Zeeman effect with the Rashba spin-orbit interaction offers an unprecedented control over the electron spin polarization. The magnetic field induces characteristic oscillations of the electron spin polarization, depicted in Fig. 3, with their amplitude and period depending on the ratio $\nu = \Delta/E_{\text{so}}$. The most promising realm for the operation of such a spin control device appears to be for Zeeman fields $E_{\text{so}} \ll \Delta \ll E_F$. Furthermore, given the typical value of the spin-orbit interaction reported for the InGaAs/InAlAs interface[16], we obtain the optimal value of the magnetic field $B \sim 5$ T that is certainly well accessible experimentally.

The effect of the electron-electron interaction in the Datta-Das setup can be potentially interesting [6, 23] and will be a subject of a future work. Equally, study of the effect of the higher transversal subbands [20] on the conductance in the Zeeman field seems worthwhile.

A.H.N. acknowledges the support of FQRNT and K.L.H. was supported by CIAR, FQRNT, and NSERC.

* E-mail: nevidomskyy@cantab.net

- [1] D. D. Awschalom, D. Loss, and N. Samarth, eds., *Semiconductor spintronics and quantum computation* (Springer, Berlin, 2002).
- [2] C. H. Bennet and D. P. DiVicenzo, *Nature (London)* **404**, 247 (2000).
- [3] S. Datta and B. Das, *Appl. Phys. Lett.* **56**, 665 (1990).
- [4] Y. A. Bychkov and E. I. Rashba, *JETP Lett.* **39**, 78 (1984).
- [5] J. C. Egues, G. Burkard, and D. Loss, *Phys. Rev. Lett.* **89**, 176401 (2002).
- [6] P. Devillard, A. Crépieux, K. I. Imura, and T. Martin, *Phys. Rev. B* **72**, 041309(R) (2005).
- [7] L. Serra, D. Sánchez, and R. López, *Phys. Rev. B* **72**, 235309 (2005).
- [8] H. Lee and S.-R. Yang, *Phys. Rev. B* **72**, 245338 (2005).
- [9] Y. Aharonov and D. Bohm, *Phys. Rev.* **115**, 485 (1959).
- [10] A. G. Aronov and Y. B. Lyanda-Geller, *Phys. Rev. Lett.* **70**, 343 (1993).
- [11] L. D. Landau and E. M. Lifshitz, *Quantum mechanics* (Pergamon Press, Oxford, 1991).
- [12] B. Das, S. Datta, and R. Reifenberger, *Phys. Rev. B* **41**, 8278 (1990).
- [13] G. L. Chen *et al.*, *Phys. Rev. B* **47**, 4084 (1993).
- [14] G. Dresselhaus, *Phys. Rev.* **100**, 580 (1955).
- [15] J. Luo, H. Munekata, F. F. Fang, and P. J. Stiles, *Phys. Rev. B* **41**, 7685 (1990).
- [16] J. Nitta, T. Akazaki, H. Takayanagi, and T. Enoki *Phys. Rev. Lett.* **78**, 1335 (1997).
- [17] T. Hassenkam *et al.*, *Phys. Rev. B* **55**, 9298 (1997).
- [18] A. V. Moroz and C. H. W. Barnes, *Phys. Rev. B* **60**, 14272 (1999).
- [19] M. Governale and U. Zulicke, *Solid State Communications* **131**, 581 (2004).
- [20] J. C. Egues, G. Burkard, and D. Loss, *App. Phys. Lett.* **82**, 2658 (2003).
- [21] The spins in the leads are assumed to be collinear, for the treatment of non-collinear lead magnetizations see e.g., M. H. Larsen, A. M. Lunde, and K. Flensberg, *Phys. Rev. B* **66**, 033304 (2002).
- [22] For the case $E_{\text{so}} \gg \Delta$, the transmission in the equal-spin channel is

$$T_{\uparrow\uparrow} = \frac{4(1-\nu)^2 F(\theta_R)^2}{c^2(1-\nu)^2 - 2c(1-\nu)P(\theta_R, \nu) + |Q(\theta_R, \nu)|^2},$$

where the auxiliary functions F , P and Q depend on the Rashba angle $\theta_R \equiv k_R L$ and angle $\phi \equiv k_0 L (1 + \varepsilon_{\text{so}})$ as

$$\begin{aligned} F(\theta_R) &= b \cos \phi \sin \theta_R + c \sin \phi \cos \theta_R \\ P(\theta_R, \nu) &= a \cos 2\phi + (b^2 + c^2 \nu) \cos 2\phi \cos 2\theta_R \\ &\quad - b c (1 - \nu) \sin 2\phi \sin 2\theta_R \\ Q(\theta_R, \nu) &= a + \frac{1}{2} [e^{i2\phi} (b + c)(b - c\nu) + \\ &\quad + e^{-i2\phi} (b - c)(b + c\nu)], \end{aligned}$$

where the following notations have been used:

$$\begin{aligned} a &= (1 - \gamma_1^2)(1 - \gamma_2^2), \quad b = \gamma_1 + \gamma_2, \quad c = 1 + \gamma_1 \gamma_2 \\ \gamma_{1,2} &= \frac{\varkappa}{k_{1,2}} = \frac{\nu}{4} \frac{k_R}{k_0(1 + \varepsilon_{\text{so}} \mp \beta)} \equiv \frac{\nu \beta}{4(1 + \varepsilon_{\text{so}} \mp \beta)}. \end{aligned}$$

- [23] V. Gritsev, G. Japaridze, M. Pletyukhov, and D. Baeriswyl, *Phys. Rev. Lett.* **94**, 137207 (2005).